

Supplementary information to “Phosphoglycerate kinase acts as a futile cycle at high temperature”

September 28, 2017

1 Model adaptation

In [1] we presented the enzyme kinetic parameters of the PGK, GAPDH, TPI and FBPA/ase of *Sulfolobus solfataricus* determined using purified enzymes and *in vitro* enzyme assays. The model was validated in its prediction of the conversion rate of 3PG to F6P and the dynamics for DHAP and GAP. As was indicated in [1], there is a large uncertainty on the BPG kinetic parameters, since we had to rely on coupled enzyme assays for the production of BPG because the compound is not commercially available. For the same reason we could not measure the half-life time of BPG at 70°C directly and had to estimate the degradation constant from published values at 60°C. Additionally, in [1] we used a HEPES/KOH buffer for the characterization of the GAPDH and we found out later that the buffer type has a profound effect on the enzyme kinetics. Since all incubations are made in Tris/HCl buffer, we made a new characterization for GAPDH kinetics. All data and model files are available on the FAIRDOMHub at <https://fairdomhub.org/investigations/156>.

1.1 GAPDH characterization in Tris/HCl buffer

In [1] we characterized the GAPDH in a HEPES/KOH buffer, which proved to yield significantly different kinetic data compared to the Tris/HCl buffer that was used in the reconstituted *in vitro* system. Since we used relatively high GAPDH concentrations (compared to PGK) in the original publication, changes in GAPDH kinetics did not result in large effect on model simulations for those incubations. However, when we tested later incubations with lower GAPDH concentrations we noticed significant differences between model simulations and experimental data.

For these reasons we decide to characterize the *S. solfataricus* GAPDH in the Tris/HCl buffer system that is also used for the reconstituted *in vitro*

system. Since we did not observe any sigmoidal saturation kinetics we could use a simpler rate equation for the enzyme:

$$v_{GAPDH} = \frac{\frac{V_{Mf} \cdot (BPG \cdot NADPH)}{K_{M,BPG} \cdot K_{M,NADPH}} - \frac{V_{Mr} \cdot (Pi \cdot GAP \cdot NADP)}{(K_{M,Pi} \cdot K_{M,GAP} \cdot K_{M,NADP})}}{\left(1 + \frac{NADP}{K_{M,NADP}} + \frac{NADPH}{K_{M,NADPH}}\right) \left(\frac{BPG}{K_{M,BPG}} + \left(1 + \frac{GAP}{K_{M,GAP}}\right) \left(1 + \frac{Pi}{K_{M,Pi}}\right)\right)}$$

resulting in the fit shown in Suppl. Fig. 1.

BPG is not commercially available and we used a preincubation of PGK with 3-PG and ATP to produce BPG. We assumed an equilibrium concentration of BPG for the incubation. The following kinetic parameters were estimated for GAPDH:

Supplementary Table 1: Kinetic parameters for Sso-GAPDH

	Estimate	Standard Error	Units
V_{Mf}	23.40	3.01	U/mg
V_{Mr}	35.87	5.15	U/mg
$K_{M,GAP}$	3.09	1.01	mM
$K_{M,NADP}$	0.20	0.046	mM
$K_{M,Pi}$	112.4	33.94	mM
$K_{M,BPG}$	$28.46E - 5$	$6.51E - 5$	mM
$K_{M,NADPH}$	0.09	0.03	mM

We also adapted the kinetic parameters for the PGK reaction, using the original data set, but not assuming complete conversion of GAP to BPG, but assuming equilibrium for the reaction. For completeness we give the original rate equation:

$$v_{PGK} =$$

$$\frac{V_{Mf} \cdot \frac{ATP \cdot 3PG}{K_{M,ATP} \cdot K_{M,3PG}} - V_{Mr} \cdot \frac{ADP \cdot BPG}{K_{M,ADP} \cdot K_{M,BPG}}}{\left(1 + \frac{ADP}{K_{i,ADP}}\right) \cdot \left\{1 + \frac{3PG}{K_{M,3PG}} \cdot \left(1 + \frac{ATP}{K_{M,ATP}}\right) + \frac{BPG}{K_{M,BPG}} \cdot \left(1 + \frac{ADP}{K_{M,ADP}}\right)\right\}}$$

with the newly fitted parameter values in Suppl Table 2.

1.2 KmBPG for PGK and GAPDH

In the original manuscript [1], we always used incubations with a large surplus of GAPDH compared to PGK and as a result the BPG binding constants were not critically tested in the validation experiments. Although we made significant improvements in the estimations of the binding constants for BPG by analysing the enzymes in the assay buffer and by not assuming

Supplementary Table 2: Kinetic parameters for Sso-PGK

	Estimate	Standard Error	Units
V_{Mf}	17.21	3.56	U/mg
V_{Mr}	37.96	13.73	U/mg
$K_{M,ADP}$	0.37	0.21	mM
$K_{M,BPG}$	$9E - 3$	$18E - 3$	mM
$K_{i,ADP}$	1.02	0.40	mM
$K_{M,ATP}$	9.31	4.64	mM
$K_{M,3-PG}$	0.57	0.45	mM

complete turnover of substrate to BPG, there are still large assumptions in the estimation, i.e. assuming equilibrium concentrations of BPG. In the experiments described in the current manuscript we made extensive variations in the PGK/GAPDH ratios, resulting in much higher BPG concentrations during the conversions. The model with the estimated BPG binding constants was not able to correctly predict these conversion experiments and we needed to fit new values for these binding constants. For this we used data from the original conversion assay in [1] and an additional new experiment with much lower GAPDH/PGK ratios.

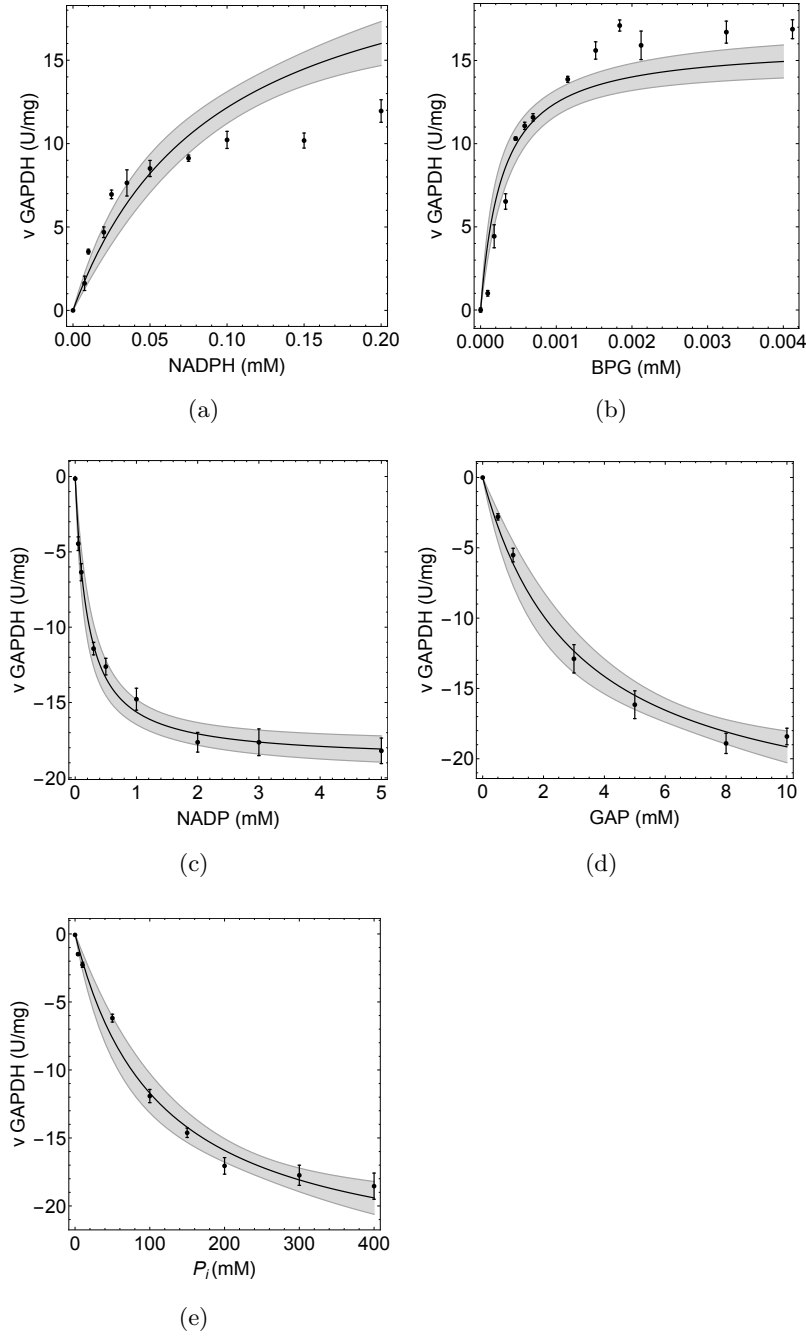
For the fits we only allowed the binding constants for BPG of PGK and GAPDH to be changed, all the other parameters were kept at their original values. The fits resulted in strongly different binding constants (KmBPG for PGK of 0.008 mM and KmBPG of GAPDH of 0.09 mM), indicating that the *in vitro* estimation with coupled enzyme assays for the generation of BPG were not precise. As a validation experiment for these binding constant we predicted the dynamics of an incubation of PGK and GAPDH. In Supplementary Figure 2 we show the model fits (a-d) and predictions (e-f).

1.3 PGK incubation at 70°C

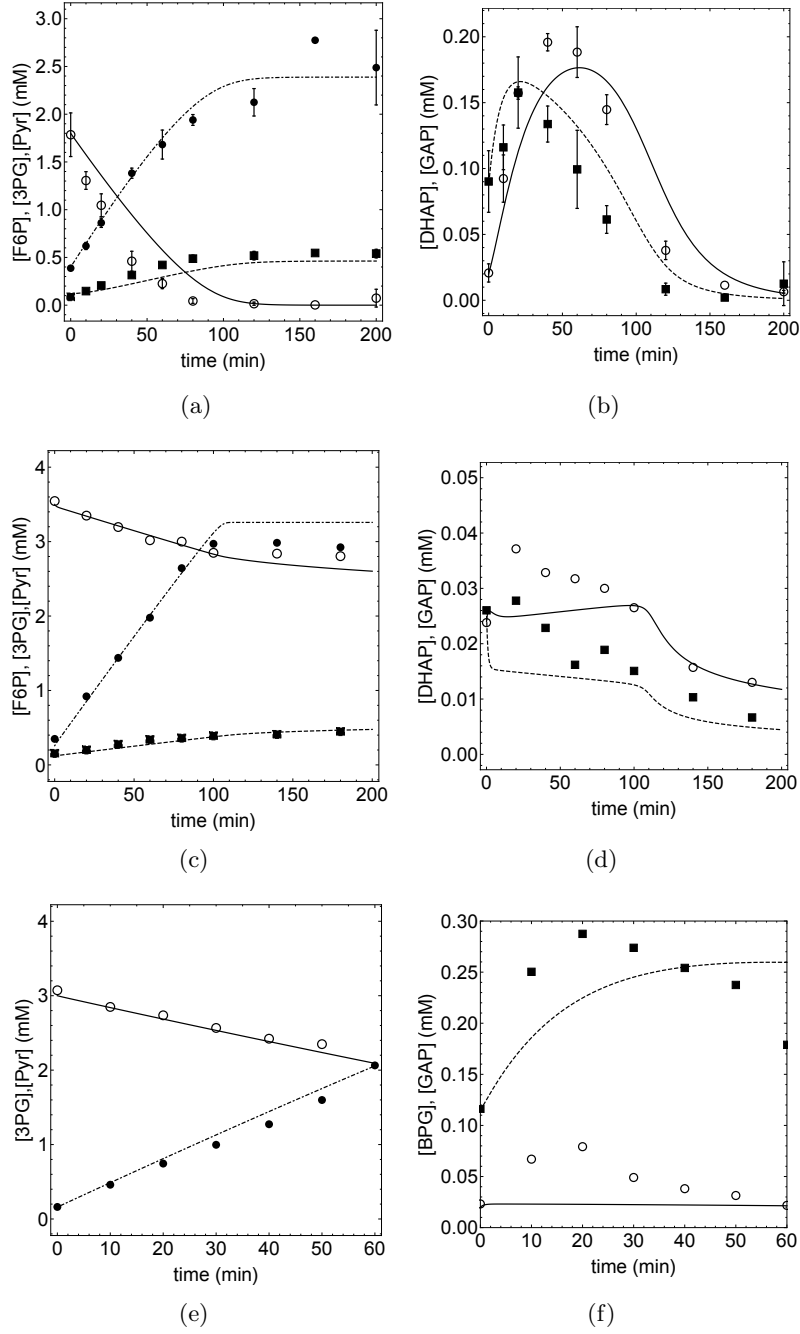
The *S. solfataricus* PGK (14 μ g/ml) was incubated at 70°C in the presence of 3-PG (5 mM), ATP (10 mM) and an ATP recycling system (5 mM PEP, 100 μ g/ml pyruvate kinase (rabbit muscle)). Any 3-PG conversion to BPG is negated by BPG degradation, keeping the 3-PG and BPG concentrations constant, with a net hydrolysis of ATP, which can be monitored by pyruvate production via the ATP recycling mechanism (see Fig. 3b). This figure accompanies Fig. 3d in the main text, and shows that halving the PGK concentration only leads to a 25% decrease in ATP hydrolysis rate.

References

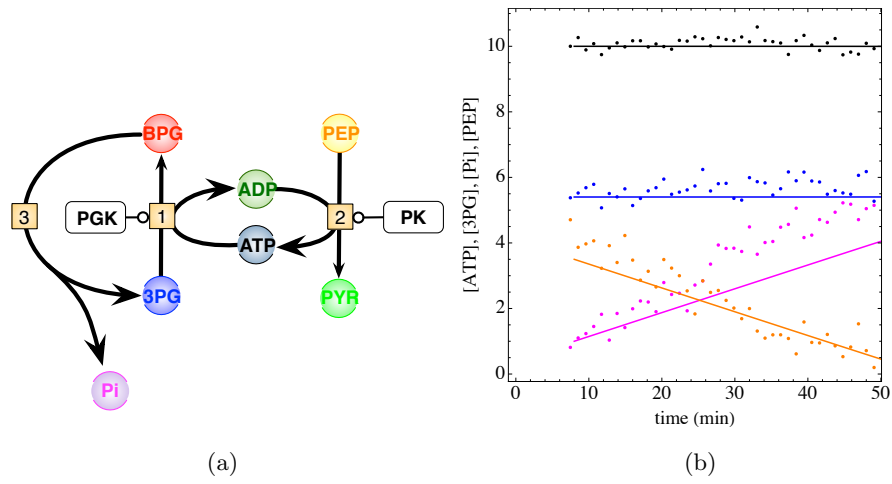
- [1] Kouril T, Esser D, Kort J, Westerhoff HV, Siebers B, et al. (2013) Intermediate instability at high temperature leads to low pathway efficiency for an *in vitro* reconstituted system of gluconeogenesis in *Sulfolobus solfataricus*. FEBS J 280: 4666-4680.



Supplementary Figure 1: GAPDH activity as a function of its substrate and product concentrations, at 70 °C. The conversion of BPG to GAP was chosen as the forward direction of the enzyme (positive rate). The drawn line is the best fit of the rate equation (Eqn 1) to all data points. Standard assay conditions (see Materials and methods) were chosen for the metabolite concentrations that were not varied. BPG is unstable and not commercially available; we could only vary its concentration indirectly by changing 3-PG concentrations in a PGK linked assay. Error bars denote the standard deviation; measurements were performed in triplicate.



Supplementary Figure 2: Fitting and validation of BPG binding constants of GAPDH and PGK. Panels a and b show the original data set of [1] for [3-PG] (open circle, and solid line for simulation), [Pyr] (filled circle, and dash-dotted line for simulation) and [F6P] (filled square, and dashed line for simulation) in panel a, and [DHAP] (open circle, solid line for simulation) and [GAP] (filled square, dashed line for simulation) in panel b with the newly fitted KmBPG values for the model simulations. Panels c and d show an additional data set that was used for fitting KmBPG and the respective simulations (same symbols and line types as in panels a and b). Panels e and f show the results for a PGK-GAPDH incubation that was used for validation of the newly fitted KmBPG values; i.e. the data were not used for fitting. Same symbols and line types as before, except for panel f where open circles denote [BPG]. The enzyme concentrations ($\mu\text{g/ml}$) in the different incubations were for panels a and b: PGK, 3.4; GAPDH, 42.1; TPI, 0.85; FBPA/ase, 3.6; for panels c and d: PGK, 4.6; GAPDH, 1.6; TPI, 5.78; FBPA/ase, 34.8; and for panels e and f: PGK 5.0; GAPDH 5.0. All simulations can be reproduced with the model kouril9.xml.



Supplementary Figure 3: PGK reaction at 70°C. In Fig. 3a the reaction network for the system is shown; reaction 1 is catalysed by the PGK, reaction 2 is the ATP recycling reaction (PK), and reaction 3 is the thermal degradation of BPG. ^{31}P -NMR spectra were analysed to follow changes in the concentrations of 3-PG (blue symbols), ATP (black symbols), PEP (orange symbols), and phosphate (pink symbols) for *S. solfataricus* PGK (28 $\mu\text{g}/\text{ml}$). The lines (coloured correspondingly to the symbols) show the model predictions for the respective conditions (see Material and Methods and Supplementary Information for details). The simulations can be reproduced with the model kouril6.xml.